Formation of a Dispersed Soil Arch in Embankments Supported by Columns with Cap Beams and the Development of System Efficacy

Karol Brzeziński, Ph.D.[1]; Kazimierz Józefiak[2]; and Radoslaw L. Michalowski, Ph.D., F.ASCE[3]

[1]Faculty of Civil Engineering, Warsaw Univ. of Technology, Warsaw, Poland.
Email: k.brzezinski@il.pw.edu.pl
[2]Faculty of Civil Engineering, Warsaw Univ. of Technology, Warsaw, Poland.
Email: k.jozefiak@il.pw.edu.pl
[3]Dept. of Civil and Environmental Engineering, Univ. of Michigan, Ann Arbor, MI.
Email: rlmich@umich.edu

ABSTRACT

The process credited for high efficacy of embankment pile support systems is the formation of soil arches in the embankment fill. The specific system considered in this presentation is one with cap beams over rows of columns inserted through soft clay to support an embankment fill. Such a system lends itself to a two-dimensional analysis. A formation of distinct arches, as conjectured in many design approaches, was not confirmed. However, based on the calculated stress distribution and the major principal stress trajectories, one can identify "dispersed" arches spanning the distance between two neighboring cap beams. The dispersed arching was not identified in low embankments, whereupon the settlement of the soft soil, a collapse mechanism propagated through the entire embankment height causing differential settlement of the embankment crown. This study was focused on the efficacy of the pile support system and on better understanding of the mechanisms behind the differential settlement at the crown of the embankment.

INTRODUCTION

Pile support systems are often used in transportation infrastructure when crossing areas with soft soils (Michalowski et al. 2018). The load from an embankment is transferred to the piles (or columns), which rest on more competent soil deposits. An investigation into the arching process, and the development of efficacy of the system was carried out using finite element analysis.

The early studies of piled embankments started in the 1980's (e.g., Reid and Buchanan 1984). The soil arching was credited for the high efficacy numbers, and the computational model suggested by Hewlett and Randolph (1988) for calculating efficacy was then repeated in many varieties for the purpose of design (e.g., Low et al. 1994; Abusharar et al. 2009, Van Eekelen et al. 2013). Numerical and semi-empirical approaches were used to study different aspects of the system (e.g., Han and Gabr 2002; Filz et al. 2012), the latter focusing on the practical aspects of the pile support systems. Soil arching was considered in many contexts in the literature (Terzaghi 1943; Ladanyi and Hoyaux 1969; Michalowski and Park 2004; Nadukuru and Michalowski 2012), and piled embankments is a subject where the design hinges on the efficacy of the system directly dependent on the soil arching phenomenon. More recent literature has focused on better understanding of the mechanism of load transfer, arching formation, and the limit state beneath what might be considered a diffused soil arch (King et al. 2019; Brzeziński and Michalowski 2021).

The study presented in this paper was focused on using a numerical method in the search for soil arching formation in the embankment fill, and on evaluating the usefulness of the method to assess the efficacy of the column support system (with cap beams) and the critical height of embankments.

PROBLEM STATEMENT

The embankment and the column support system is assumed to have a periodic structure, Fig. 1(a), and the numerical analysis will include one symmetric half of the periodic cell, Fig. 1(b).

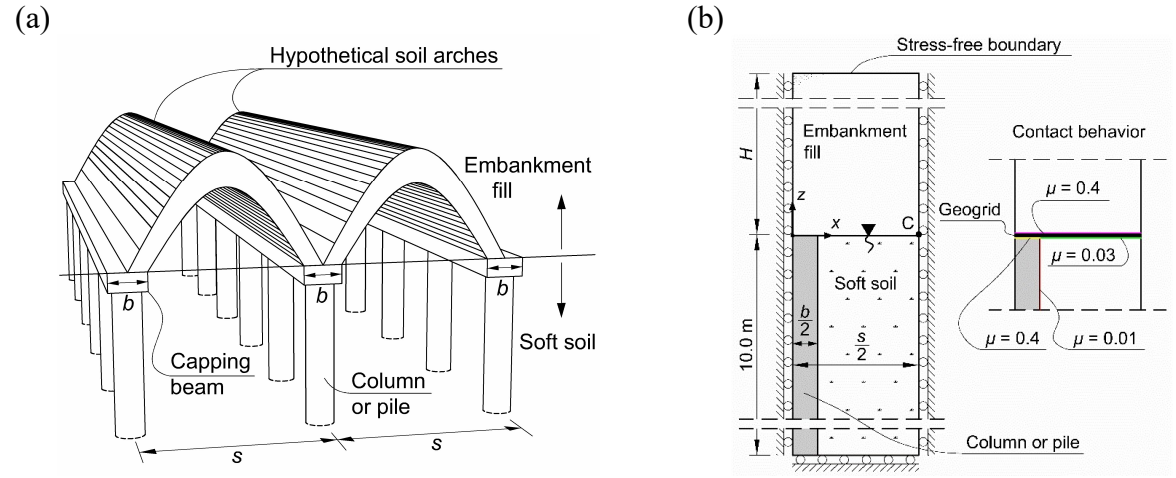

Figure 1. Problem definition: (a) hypothetical formation of soil arches, and (b) symmetric half of the periodic cell and the boundary conditions.

The boundary conditions are illustrated in Fig. 1(b). Because the columns are spanned by capping beams, the problem is reduced to a 2D problem, with the columns approximated by a wall with negligible friction on the interface with soft soil (friction coefficient $\mu = 0.01$). The soft soil is a permeable elastic material ($E = 1.0$ MPa, $\nu = 0.3$, hydraulic conductivity $k = 3.5 \cdot 10^{-8}$ m/s, unit weight $\gamma = 17.0$ kN/m^3, void ratio $e = 1.3$). The upper surface of the soft soil is a permeable (draining) boundary, whereas the vertical and the bottom boundaries are impermeable.

The embankment soil is elastic-plastic with strength governed by the Mohr-Coulomb criterion and deformation governed by the non-associative plastic flow rule ($E = 60.0$ MPa, $\nu = 0.3$, $\phi = 40°$, dilatancy angle $\psi = 10°$, cohesion $c = 0.1$ kPa, unit weight $\gamma = 19.0$ kN/m^3). Columns are linear elastic ($E = 27.0$ GPa, $\nu = 0.16$, unit weight $\gamma = 24.0$ kN/m^3), and so is the geogrid ($E = 10.0$ GPa, $\nu = 0.30$, unit weight $\gamma = 10.0$ kN/m^3). The geogrid was modeled as a bar (or truss element) with tensile stiffness.

Spacing of columns was taken in all computations as $s = 2.0$ m and the width of the cap beam was $b = 0.4$ m. Computations were carried out using the finite element system Abaqus (2011).

CONSOLIDATION OF THE WEAK SOIL

The embankment is constructed in half-meter thickness layers (lifts). Each layer is placed in a 10-min period, and the process of soft soil consolidation follows for 7 days under constant

load, before the next layer is placed. The construction process of a 3-m embankment is illustrated in Fig. 2(a). Seven-day intervals, A through F, are illustrated in the figure, with the continuing process reaching 407 days, i.e., a 42-day construction period plus 365 days of consolidation under constant load. The load transfer platform (LTP) has one layer of geogrid reinforcement.

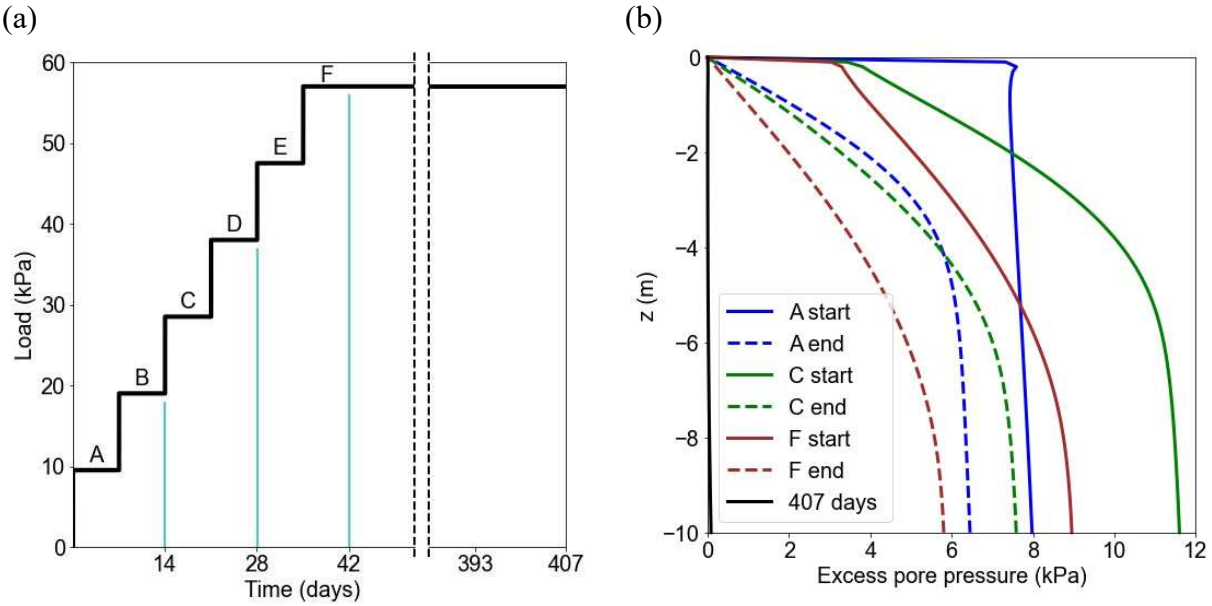

Figure 2. Consolidation process of the soft soil: (a) embankment load as a function of time, and (b) pore water pressure beneath point C (in Fig. 1(b)) at selected times.

The excess pore water pressure distribution in the weak soil beneath point C (Fig. 1(b)) during the layered construction of the embankment is illustrated in Fig. 2(b) at the beginning and end of intervals A, C and F, and after 365 days following the end of embankment construction (a total of 407 days).

It is not surprising that upon application of the first-lift load on the soft soil, the excess pore water pressure increases almost uniformly throughout the entire soft soil depth (solid blue line in Fig. 2(b)). During the following 7-day consolidation interval the pore water drains through the upper boundary of the soft soil to assume the distribution depicted by the dashed blue line. When the third lift of soil is placed at 14 days, the excess pore water pressure increases to that illustrated by the solid green line, and it dissipates during the following time interval C to assume distribution shown by the dashed green line at 21 days. The process is repeated until interval F ending on day 42. In the following 365 days the excess pore water pressure is practically nil.

SETTLEMENT AND SHEAR STRAINS IN EMBANKMENT FILL

Vertical displacement increments during construction of a 3-m embankment are shown in Fig. 3 (a,b,c). Each of the graphs shows displacements in the upper portion of a half of the periodic cell, Fig. 1(b), during intervals A, C and F depicted in Fig. 2(a). The extent of the capping beam is depicted by a thick gray line in the lower left of all graphs. The largest displacement increments during the construction phase occurred in the first 7-day interval (interval A in Fig. 2(a)), with a red block moving downward by several millimeters, Fig. 3(a).

The soil above the capping beam, however, seems to have moved by an amount close to zero (dark blue), producing a shear band between the two regions. This shear band is shown in Fig. 3(d) as hashed region (shear strain beyond the color scale used in the figure).

During interval C the spread of vertical displacement increments is much smaller, Fig. 3(b), but the differential settlement still reaches the top surface of the embankment constructed to the height of 1.5-m. During the last interval (F) the displacement increments are much more uniform, no shear band reaches the top surface, Fig. 3(f), and no differential settlement occurs on the surface of the constructed embankment, Fig. 3(c).

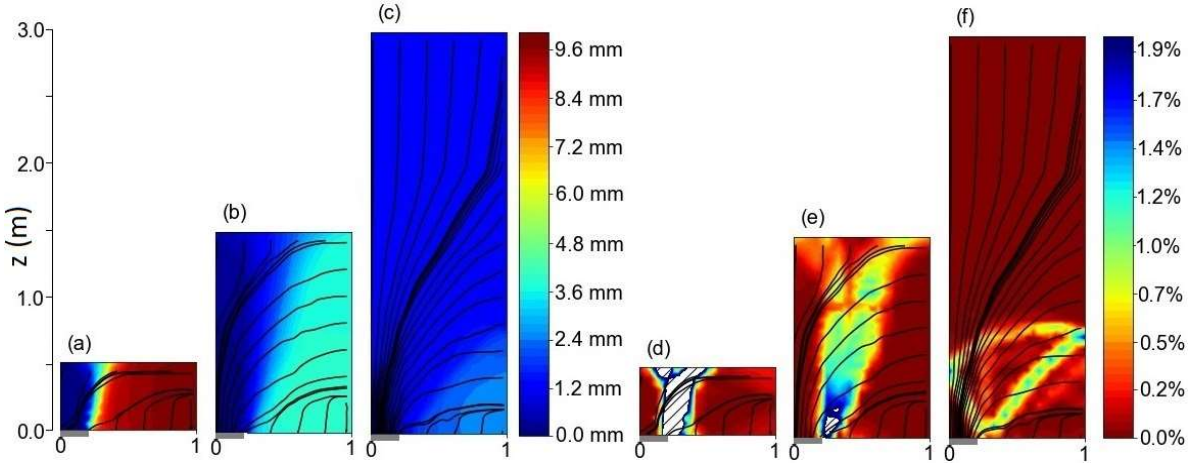

Figure 3. Construction sequence for a 3-m embankment with reinforced LTP: (a, b, c) vertical displacement increments during 7-day intervals A, C, F (Fig. 2(a)), and (d, e, f) maximum shear strain increments during 7-day intervals A, C, F.

The black lines superimposed on the graphs in Fig. 3 are the trajectories of major principal stresses. Their distribution in Fig. 3(c,f) seems to suggest the transfer of load to the capping beam and possible arch formation above the shear bands in Fig. 3(f). Those shear bands are indicative of a failure mechanism (plastic deformation) in the lower portion of the embankment fill, and they resemble the inverted kinematic discontinuities associated with the Prandtl (1920) static solution to a punch indentation problem.

DISPERSED ARCHING

Soil arching is a phenomenon induced by disparities in structural support stiffness and it is manifested in a pattern of stress distribution as opposed to the kinematics, which is more indicative of the failure mechanism, particularly in the presence of strain localization.

In order to investigate soil arching in embankment fill, the distribution of principal stress ratio σ_3/σ_1 is plotted in Fig. 4(a) while in-plane mean stress $(\sigma_1 + \sigma_3)/2$ is shown in Fig. 4(b). Ratio $\sigma_3/\sigma_1 = 1$ (dark red) in the first graph indicates isotropic stress. Two small isotropic stress regions are found along the symmetry plane of the periodic cell, at the level of about 1.5 and 1.9 m, which is something of a peculiarity (the small red region at the top boundary is likely to be a numerical consequence of the stress-free condition). However, it explains the diversion of the major principal stress directions in Fig. 3(c,f) along the model symmetry plane from being horizontal in the lower portion, to vertical in the upper portion of the embankment.

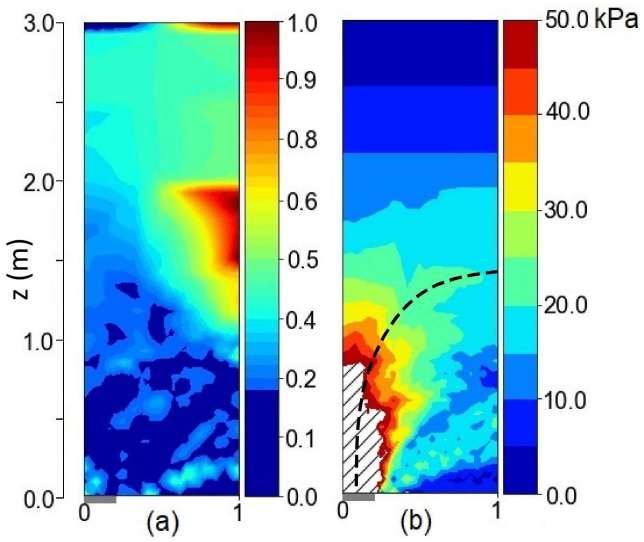

Figure 4. Stress distribution in 3-m embankment with reinforced LTP: (a) principal stress ratio σ_3/σ_1, and (b) in-plane mean stress.

The dark-blue in Fig. 4(a) indicates the embankment fill reaching the failure state, whereas the light-blue through red shows the elastic state with increasing distance from the failure criterion. The sense of the stress magnitude is given by the in-plane mean stress in Fig. 4(b). The hashed area directly above the capping beam (lower left) is stressed beyond 50 kPa.

The distribution of the in-plane mean stress indicates a region with elevated stresses along the black dashed line in Fig. 4(b). This line coincides approximately with the major principal stress trajectory shown in Fig. 3(c). One could envision a wide band region along the dashed line with the darker blue above and below denoting lower stresses. This might give rise to the conjecture of a dispersed (or diffused) soil arch. The center of this presumed arch at the symmetry of the model appears to be just below the region with the isotropic stress state. This feature in the stress field was noticed in a previous study (Brzeziński and Michalowski 2021), but now the same feature is detected in the sequentially (in layers) built embankments with geosynthetic reinforcement used in the load transfer platform.

SYSTEM EFFICACY DRIVEN BY THE CONSOLIDATION OF THE SOFT BASE

Efficacy

The efficacy of the system is defined as a ratio of the load transferred to the columns to the total embankment load, and it can be calculated for half of the periodic cell as

$$E_f = \frac{2\int_0^{b/2} \sigma_{zz}\, dx}{\gamma s h} \tag{1}$$

where s and b are the column spacing and the cap beam width, respectively, γ is the unit weight of the embankment fill, and h is the constructed embankment height (increasing with

construction time), and the final h is equal to design height H. Stress σ_{zz} is the vertical stress component on the capping beam. The definition of efficacy in Eq. (1) is suitable for a system with capping beams. i.e., a system that can be considered with a 2D analysis. Essentially, the numerator represents the load transmitted to the cap beam while the denominator is the embankment weight (load) in the periodic cell.

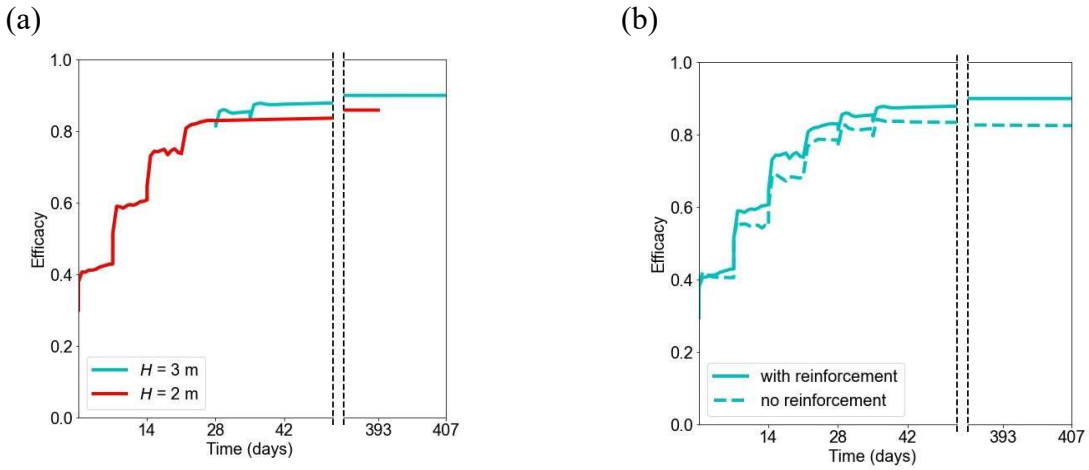

Figure 5. Development of efficacy as a function of time: (a) embankments of 2- and 3-m height with reinforced LTP, and (b) 3-m high embankment (with and without reinforcement in LTP).

The efficacy develops as a function of soft soil settlement, which is a function of the consolidation process of the weak subsoil. Consequently, the efficacy is a function of construction time; this process is illustrated in Fig. 5. A comparison of the efficacy developed for 2- and 3-m embankments (both with reinforcement in LTP) is illustrated in Fig. 5(a). After the first half-meter lift is placed, the calculated efficacy sets at 0.379. After the next 7 days the efficacy increases to 0.429, and with the next lift of the fill it surges to 0.608. The process is repeated twice more and the embankment reaches the final height of 2.0 m. Every time a new lift is placed the efficacy increases, but by a lesser amount. After placing the four lifts of the fill and allowing the soft soil to consolidate another 7 days (total construction time of 28 days), the efficacy increased to 0.830; in the next 365 days, the efficacy stabilized at 0.858 (total time 393 days). The process for the 3-m embankment is identical in the first four intervals, but the efficacy dips by a small amount when a new lift is placed, followed by an increase. When the embankment height reached 3 m, the efficacy reached 0.875 (at 42 days), and increased to 0.900 after the following 365 days. The higher the embankment, the smaller the efficacy increase produced by the next lift.

A 3-m embankment constructed without reinforcement in LTP (dashed line in Fig. 5(b)) mobilizes the efficacy of 0.835 (at 42 days), a small drop from the embankment with reinforced LTP, and after the following 365 days it stabilized at a slightly diminished value of 0.825. Not surprisingly, the reinforcement enhances the performance of the column support system.

The efficacy reported with three digits after the decimal point is not to suggest the precision capabilities of the model; it is only for future purposes of comparison.

Force in reinforcement

The reinforcement was modeled as an elastic bar with tensile stiffness. The coefficient of friction of the embankment fill over the reinforcement was $\mu = 0.4$, and so was the friction coefficient of the reinforcement over the pile capping beam. The coefficient of friction of reinforcement over the soft soil was taken as $\mu = 0.03$.

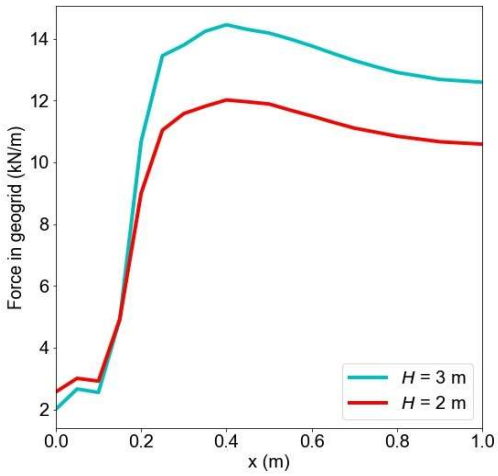

Figure 6. Force in LTP reinforcement for 2- and 3-m tall embankments.

The force in the reinforcement varies during the embankment construction, and the force distribution at 365 days after embankment construction are shown in Fig. 6 for 2- and 3-m embankments.

As expected, the maximum tensile force in the reinforcement increases with an increase in the embankment height. For the specific geometry of the system used in computations (column spacing $s = 2.0$ m, width of cap beam $b = 0.4$ m), the force in the reinforcement increases significantly near the edge of the capping beam, to reach a maximum at about half of the cap beam width from the edge of the beam. The force then drops slightly with increasing distance away from the columns. The force is dependent on the reinforcement stiffness, but an investigation of the relationship between the force and stiffness of the reinforcement was not part of this study.

DIFFERENTIAL SETTLEMENTS AND CRITICAL EMBANKMENT HEIGHT

The second important piece of information for design purposes, next to system efficacy, is the critical height of embankments. The critical height is defined as the minimum height that prevents the differential settlements from propagating to the embankment surface. A question that was asked in the study was: how effective is one layer of reinforcement in preventing differential settlements at the embankment crown?

Computational results for 2- and 3-m tall embankments with and without reinforcement are illustrated in Fig. 7. The ordinate represents the differential vertical displacements and the abscissa shows the elevation in the embankment. Elevation $z = 0$ is the level of the interface of the embankment fill with the soft soil (with or without reinforcement), whereas $z = H$ is the level

of the embankment crown. The lines in red are used for results of the 2-m embankment and the turquoise is used for the 3-m embankment; solid lines are for cases with reinforcement in the load transfer platform, and dashed lines for no reinforcement.

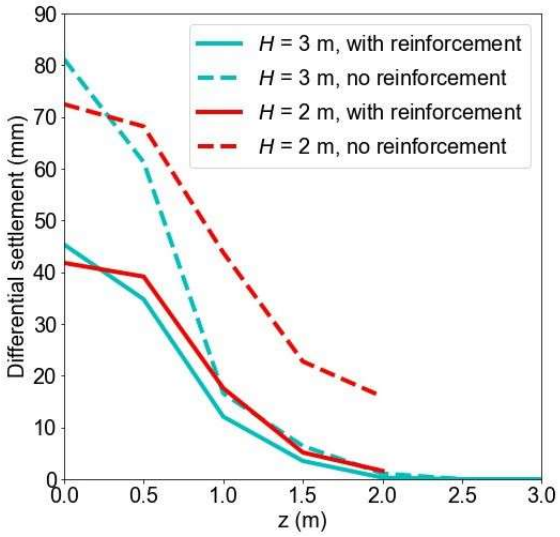

Figure 7. Differential settlements.

The 2-m embankment without reinforcement (dashed-red) shows about 16 mm of differential settlement at the crown ($z = H = 2.0$ m), but the differential vertical displacement is even larger for lower elevations, 72.5 mm at $z = 0$. When reinforcement is used, the differential vertical displacement drops to 41.8 mm, and the calculated differential settlement on the embankment surface is only 1.6 mm. Hence the use of reinforcement has a significant influence on the critical height. A 3-m embankment shows no differential settlement at the crown ($z = 3$ m) whether or not reinforcement was used (the critical embankment height for this model appears to be about 2.5 m).

An interesting outcome is that the differential vertical displacements within the embankment in the proximity of the fill-soft base interface ($z = 0$) are smaller for the lower embankment. This trend, however, is quickly reversed with an increase in z. The differential settlement at $z = 0$ was taken as the difference between the largest settlement of the soft soil and the settlement of the cap beam placed over the columns. Typically, the settlement of columns is small, whereas the magnitude of the soft soil settlement increases significantly with the embankment height. This is the likely cause of the peculiar outcome shown in Fig. 7 for elevation z close to zero.

CONCLUSIONS

Finite element analysis was found to be useful in the study of arching and the development of column support efficacy. A distinct soil arch, as those assumed in approximate design methods, was not detected, but the calculated stress field allows for formulating the conjecture of a diffused soil arch. This arch approximately follows the trajectories of major principal stresses in the embankment fill.

The efficacy of the column support system is not a constant; it varies with the settlement of the base soil, and it undergoes rapid increases as the sequential soil lifts are placed, but these

increases have a tendency to become smaller as the embankment height increases. The long-term changes in efficacy under constant load are small; the efficacy was found to be increased when reinforcement was used in the load transfer platform. For the geometry of the system and material properties considered in the study, the efficacy of a 3-m embankment stabilized at 0.90. For a 3-m embankment without reinforcement the final efficacy was found to be almost 10% lower.

The critical height of the embankment is dependent on the system geometry and material properties. While a comprehensive study of the differential settlements and the critical height was not part of this investigation, the method used clearly indicated the positive influence of the reinforcement in the load transfer platform on the differential settlements.

ACKNOWLEDGEMENTS

The work presented in this paper was supported in part by the National Science Foundation, Grant No. CMMI-1901582 and by the Dekaban Fund, administered by the University of Michigan. The support from both sources is greatly appreciated.

REFERENCES

Abaqus. (2011). *Theory Manual, Ver. 6.11*. Dassault Systèmes Simulia Corp., Providence, RI, USA, pp.1172.

Abusharar, S. W., Zheng, J.-J., Chen, B.-G., and Yin, J.-H. (2009). "A simplified method for analysis of a piled embankment reinforced with geosynthetics." *Geotextiles and Geomembranes*, 27(1), 39-52.

Brzeziński, K., and Michalowski, R. L. (2021). "Diffused arching in embankments supported by non-compliant columns with capping beams." *Computers and Geotechnics*, 132 (April), 104522 (1-12).

Filz, G., Sloan, J., McGuire, M. P., Collin, J., and Smith, M. (2012). "Column-supported embankments: settlement and load transfer." *Geotechnical engineering state of the art and practice: keynote lectures from Geo-Congress 2012*, Reston, VA, 54-77.

Han, J., and Gabr, M. (2002). "Numerical analysis of geosynthetic-reinforced and pile-supported earth platforms over soft soil." *J. Geotech. Geoenviron. Eng.*, 128(1), 44-53.

Hewlett, W. J., and Randolph, M. F. (1988). "Analysis of piled embankments." *Ground Eng.* 21(3), 12–18.

King, L., Bouazza, A., Dubsky, S., Rowe, R. K., Gniel, J., and Bui, H. H. (2019). "Kinematics of soil arching in piled embankments." *Géotechnique* 69 (11), 941–958.

Ladanyi, B., and Hoyaux, B. (1969). "A study of the trap-door problem in a granular mass." *Can. Geotech. J.*, 6(1), 1-14.

Low, B., Tang, S., and Choa, V. (1994). "Arching in piled embankments." *ASCE J. Geotech. Eng.* 120(11), 1917-1938.

Michalowski, R. L., and Park, N. (2004). "Admissible stress fields and arching in piles of sand." *Géotechnique*, 54(8), 529-538.

Michalowski, R. L., Wojtasik, A., Duda, A., Florkiewicz, A., and Park, D. (2018). "Failure and remedy of column-supported embankment: case study." *J. Geotech. Geoenviron. Eng.*, 144(3), 05017008, 1-14..

Nadukuru, S. S., and Michalowski, R. L. (2012). "Arching in distribution of active load on retaining walls." *J. Geotech. Geoenviron. Eng.*, 138(5), 575-584.
Prandtl, L. (1920). "Über die Härte plastischer Körper." Nachr. Königl. Ges. Wissensch., Göttingen, *Mathematisch-physikalische Klasse*, 74-85.
Reid, W., and Buchanan, N. (1984). "Bridge approach support piling." *Proc. Conf. on Advances in Piling and Ground Treatment*, Thomas Telford Publishing, London, 267-274.
Terzaghi, K. (1943). *Theoretical Soil Mechanics*. Wiley, New York.
Van Eekelen, S., Bezuijen, A., and Van Tol, A. (2013). "An analytical model for arching in piled embankments." *Geotextiles and Geomembranes*, 39 (August), 78-102.